

Geometry and temperature effects of the interfacial thermal conductance in copper– and nickel–graphene nanocomposites

This article has been downloaded from IOPscience. Please scroll down to see the full text article.

2012 J. Phys.: Condens. Matter 24 245301

(<http://iopscience.iop.org/0953-8984/24/24/245301>)

View [the table of contents for this issue](#), or go to the [journal homepage](#) for more

Download details:

IP Address: 18.111.85.34

The article was downloaded on 12/06/2012 at 11:42

Please note that [terms and conditions apply](#).

Geometry and temperature effects of the interfacial thermal conductance in copper– and nickel–graphene nanocomposites

Shu-Wei Chang¹, Arun K Nair¹ and Markus J Buehler^{1,2,3}

¹ Laboratory for Atomistic and Molecular Mechanics, Department of Civil and Environmental Engineering, Massachusetts Institute of Technology, 77 Massachusetts Avenue, Room 1-235A&B, Cambridge, MA 02139, USA

² Center for Materials Science and Engineering, Massachusetts Institute of Technology, 77 Massachusetts Avenue, Cambridge, MA 02139, USA

³ Center for Computational Engineering, Massachusetts Institute of Technology, 77 Massachusetts Avenue, Cambridge, MA 02139, USA

E-mail: mbuehler@MIT.EDU

Received 2 March 2012, in final form 11 April 2012

Published 18 May 2012

Online at stacks.iop.org/JPhysCM/24/245301

Abstract

Graphene has excellent mechanical, electrical and thermal properties. Recently, graphene–metal composites have been proposed as a means to combine the properties of metals with those of graphene, leading to mechanically, electrically and thermally functional materials. The understanding of metal–graphene nanocomposites is of critical importance in developing next-generation electrical, thermal and energy devices, but we currently lack a fundamental understanding of how their geometry and composition control their thermal properties. Here we report a series of atomistic simulations, aimed at assessing the geometry and temperature effects of the thermal interface conductance for copper– and nickel–graphene nanocomposites. We find that copper–graphene and nickel–graphene nanocomposites have similar thermal interface conductances, but that both cases show a strong performance dependence on the number of graphene layers between metal phases. Single-graphene-layer nanocomposites have the highest thermal interface conductance, approaching $\sim 500 \text{ MW m}^{-2} \text{ K}^{-1}$. The thermal interface conductance reduces to half this value in metal–bilayer graphene nanocomposites, and for more than three layers of graphene the thermal interface conductances further reduces to $\sim 100 \text{ MW m}^{-2} \text{ K}^{-1}$ and becomes independent with respect to the number of layers of graphene. This dependence is attributed to the relatively stronger bonding between the metal and graphene layer, and relatively weaker bonding between graphene layers. Our results suggest that designs combining metal with single graphene layers provide the best thermal properties.

(Some figures may appear in colour only in the online journal)

1. Introduction

Recent advances in the fabrication of ultrathin graphene layers have attracted a great deal of attention to study

size effects of multilayer graphene films [1–3]. Due to its remarkable physical properties such as high mechanical strength, and electrical and thermal conductivity, many studies have been devoted to the electronic structure of n -layer

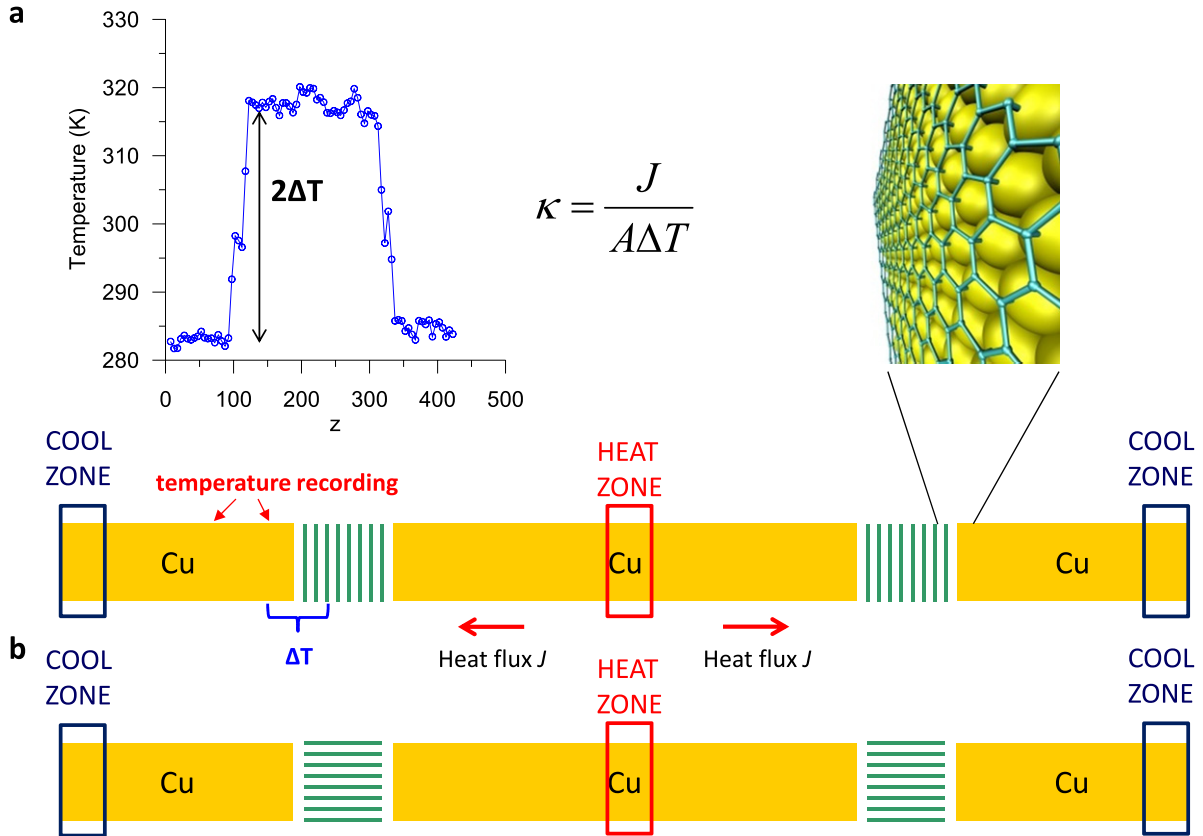


Figure 1. Illustration of the Müller-Plathe approach and geometry of the metal–graphene nanocomposite. (a) Temperature distribution of a metal–graphene nanocomposite and illustration of copper/cross-plane multilayer graphene nanocomposite. (b) Copper/in-plane multilayer graphene nanocomposite.

graphene systems [4, 5] and their vibrational properties [6–8]. Graphene nanocomposite materials have been recently studied with the aim of creating new materials with bulk quantities of graphene. However, most of the earlier studies have primarily been focused on polymer matrices [9–11] and few have been concerned with metal matrices, albeit some recent studies have focused on the synthesis and assessment of the mechanical properties of this class of materials [12–14].

Graphene–metal materials are high performance thermal interface materials [15, 16] and the understanding of thermal interface conductance between metal and graphene is crucial for the design of next-generation electronic or energy devices. However, there is limited amount of data for thermal interface conductance at the metal–graphene interface [17]. Previous studies have measured the thermal interface conductance at SiO_2 –graphene [18] and Au–graphene interfaces [8]. Schmidt *et al* have reported that the thermal interface conductances between c -axis-oriented highly ordered pyrolytic graphite and several metals, including Al, Au, Cr and Ti, in the temperature range of 87–300 K are found to be similar to those of metal–diamond interfaces in the range of 40–100 $\text{MW m}^{-2} \text{K}^{-1}$.

Here, a series of atomistic simulations, aimed at assessing the geometry and temperature effects, are performed to systematically study the thermal interface conductance between n -layer graphene ($n = 1, 2, 3, 4, 8$ and 12) and copper and nickel interfaces. We calculate and compare

the thermal interface conductance of different orientations of graphene layers (metal and in-plane graphene and metal and cross-plane graphene interfaces). Furthermore, the temperature effects on the thermal interface conductance in the temperature range of 230–430 K and the size effects on the thermal interface conductance are investigated to provide overall studies of the thermal interface conductance of metal–graphene nanocomposites.

2. Materials and methods

We consider metal and n -layer graphene ($n = 1, 2, 3, 4, 8$ and 12) nanocomposite materials as shown in figure 1. We calculate the interfacial thermal conductances at the metal–graphene interface for different orientations of graphene, temperatures, metal and the thickness of the multilayer graphene. Copper and nickel are the two metals investigated in this study. As shown in figure 1, two orientations, in-plane and cross-plane, of the graphene are studied. We fix the thickness of the metal to 20 nm and vary the number of the layers of graphene n to study the size effects of the thermal interface conductance.

Embedded-atom-method (EAM) interatomic potentials [19], which include electron density contributions of atoms, are used for describing interactions between metal atoms. The interatomic interactions in graphene sheets are

described using the adaptive intermolecular reactive empirical bond-order (AIREBO) potential [20], which is parameterized for carbon and/or hydrogen atoms. Additionally, Lennard-Jones (LJ) potentials are used to model the interactions between metals and graphene sheets. The choice of the pair potential is motivated by previous results that have indicated that the LJ potential with parameters derived from quantum level simulations provides a reasonable approximation to the behavior of metal–carbon interactions [21]. The LJ potential used here is suitable for this study since bonding between metal and graphene are van der Waals bonds and we only focus on the vibrational properties of metal–graphene nanocomposites at equilibrium configurations. We use the parameters that have been developed, tested and used in earlier studies to describe copper–graphene [22] and nickel–graphene [23] interactions.

LAMMPS is used to calculate the thermal interface conductance of metal–graphene nanocomposites [24]. For each model of the metal–graphene nanocomposites, an *NPT* ensemble is used to obtain the equilibrium structure. After *NPT* simulation, the Müller-Plathe approach [25] is used to calculate the thermal interface conductance. In the Müller-Plathe approach, a constant-energy molecular dynamics simulation (*NVE*) is performed and additional control is made through exchanging the momentum of atoms between the ‘heat zone’ and ‘cool zone’ every 1.3 ps as illustrated in figure 1. After achieving a steady state of the system, the temperature jump ΔT at the metal–graphene interface is computed and then the thermal interface conductance is calculated by

$$\kappa = \frac{J}{A\Delta T} \quad (1)$$

in which J is the heat flux and A is the cross-section area of the nanocomposites.

3. Results and discussion

We first compute the thermal interface conductance for copper and in-plane graphene and copper and cross-plane graphene interfaces as illustrated in figure 1. We find that the copper and cross-plane multilayer graphene ($n = 8$) nanocomposite has a thermal interface conductance of $84 \text{ MW m}^{-2} \text{ K}^{-1}$ while the copper and in-plane multilayer graphene ($n = 8$) nanocomposite has a larger thermal interface conductance of $230 \text{ MW m}^{-2} \text{ K}^{-1}$. We note that Gao *et al* have reported that interface thermal conductance between a metallic carbon nanotube and a Cu substrate is $296 \text{ MW m}^{-2} \text{ K}^{-1}$ [26], which is close to our predicted value for the copper and in-plane graphene case. Our results show that the interface between the face-centered cubic (fcc) metal (111) surface and the in-plane multilayer graphene has a larger thermal interface conductance. The result is reasonable as the phonon group velocity is much higher for in-plane graphite compared to out-of-plane graphite. In agreement with our finding, an extension of the diffuse mismatch model has also predicted the same trend [27]. Experimental studies, which have shown that the thermal interface conductance between an

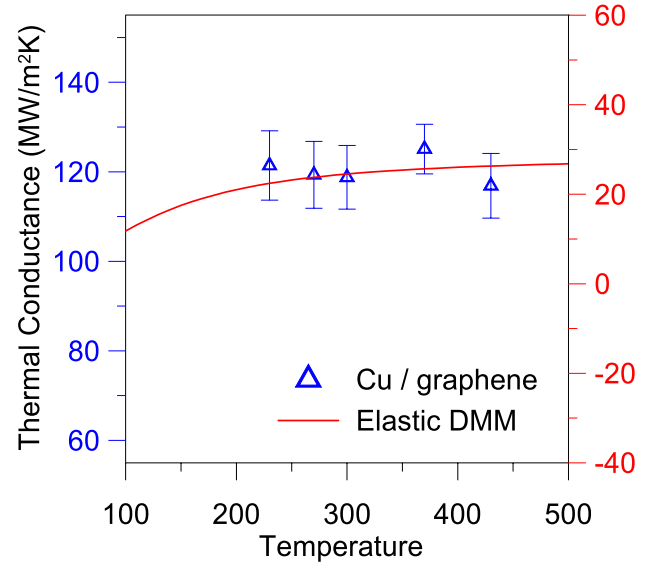


Figure 2. Temperature effects of the thermal interface conductance, including simulation results and theoretical analysis using DMM. The nanocomposite consists of 20 nm copper and four-layer graphene. The results show that there is no strong dependence between the thermal interface conductance and the temperature at temperatures above 200 K.

individual carbon nanotube (CNT) and a Au surface for *a*-axis orientation is larger than for its *c*-axis orientation [28], also support the same trend as identified in our calculations. Although the in-plane multilayer graphene has a larger thermal interface conductance, the adhesion of the cross-plane graphene on fcc metal (111) is more stable, and we thus focus on the metal and cross-plane graphene case for studying the temperature and size effects of the thermal interface conductances.

We vary the temperature and calculate the thermal interface conductance for a copper–four-layer-graphene nanocomposite. We find that in the temperature range 230–430 K the thermal interface conductance of the copper–graphene interface is about $120 \text{ MW m}^{-2} \text{ K}^{-1}$ (figure 2) and there is no strong dependence between the thermal interface conductance and the temperature. It is worth noting that our results are consistent with theoretical models [27] and experimental data [29] which have shown that the thermal interface conductance is essentially independent of temperature at temperatures above 200 K.

To quantify this, we use a modified elastic diffuse mismatch model (DMM) originally described by Duda *et al* for thermal contact between isotropic and anisotropic materials [30]. The thermal interface conductance from a metal film to a graphite substrate is given by

$$h_{\text{BD}} = \frac{1}{4} \sum_j^3 \int_{\omega_{\text{D},j}} \hbar \omega v_{1,j} D_1(\omega, v_{1,j}) \frac{\partial f}{\partial T} \zeta_{(2),j}^{1 \rightarrow \text{g},c} d\omega. \quad (2)$$

Here j is a particular polarization, \hbar is the Planck’s constant divided by 2π , ω is the phonon angular frequency, T is the temperature and f is the Bose–Einstein distribution function. The metal properties are denoted by a subscript

or superscript ‘1’. The symbol ‘g’ represents graphite, ‘c’ denotes the direction along the *c* axis of graphite, $\omega_{D,j}$ is the Debye cutoff and $\zeta_{(2),j}^{1 \rightarrow g,c}$ is the transmission coefficient from the metal film to the *c*-axis graphite. Only the elastic processes are considered here and hence

$$\zeta_{(2),j}^{1 \rightarrow g,c} = \frac{\frac{v_{c,j}}{v_{a,j}^2} \frac{1}{d}}{\frac{\omega}{v_{1,j}^2} + \frac{v_{c,j}}{v_{a,j}^2} \frac{1}{d}} \quad (3)$$

where *d* is the interlayer spacing in graphite and is taken as $d = 3.35 \text{ \AA}$. The parameter $v_{1,j}$ is the polarization-specific Debye phonon group velocity and we use the values reported in [31] for copper. For graphite, we use the same values as used by Duda *et al*, where $v_{a,1} = 23\,600 \text{ m s}^{-1}$, $v_{a,t} = 15\,900 \text{ m s}^{-1}$, $v_{c,1} = 1\,960 \text{ m s}^{-1}$ and $v_{c,t} = 700 \text{ m s}^{-1}$ [30]. The predicted thermal interface conductances are plotted in figure 2. In accordance with results from previous studies [29, 30, 32] the DMM qualitatively captures most of the temperature trend, but the DMM under-estimates the thermal interface conductance.

In order to study how the thermal interface conductance varies as the thickness of the graphene changes, we vary the number of layers of graphene *n* and calculate the thermal interface conductance for copper–graphene and nickel–graphene nanocomposites at a temperature of 300 K. Without presuming the stacking between the interface of metal and graphene, for $n = 1\text{--}3$ we construct initial models with both topfcc and hcpfcc stacking between the interface of metal and graphene. The results show that after *NPT* simulations, no matter if the initial model is topfcc or hcpfcc stacking, the stacking between the metal and graphene interface changes into hcpfcc stacking at equilibrium, indicating that the hcpfcc stacking is more stable for metal–graphene nanocomposites.

In order to validate the predictions from our molecular simulations, we compute the interface stacking sequence for graphene–copper using density functional theory (DFT) for topfcc and hcpfcc cases. A fully periodic unit cell is used with the copper atoms oriented in the (111) direction with one layer of graphene at the interface of the copper–graphene composite. The periodic system is then relaxed to find the stable stacking sequence. We use the Quantum ESPRESSO package [35] for DFT calculations with Perdew–Zunger pseudopotential parameters [33]. Energy cutoffs of 30 and 300 Ryd are used for plane-wave basis sets and charge density grids with 32 Monkhorst–Pack sampling *k*-points for Brillouin zone integration and has been verified to achieve a total energy convergence less than 1 meV/atom. Geometric relaxations are carried out for both topfcc and hcpfcc cases such that the force on atoms converged below a threshold of 10 meV \AA^{-1} . Our DFT results indicate that the hcpfcc case has a lower energy state compared to the topfcc case. This confirms the stacking sequence predicted by our molecular dynamics results and hence the hcpfcc stacking sequence obtained in the molecular simulations is not an artifact of the interatomic potential employed at the interface.

The results of thermal interface conductance for metal–graphene nanocomposites with different numbers of

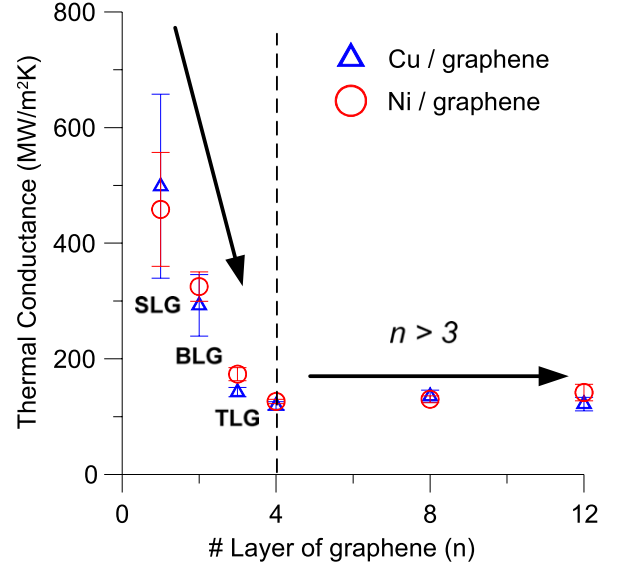


Figure 3. Size effects of the thermal interface conductance. The results show that copper/graphene and nickel/graphene nanocomposites have similar thermal interface conductance and the thermal interface conductance of metal/single-layer-graphene nanocomposite is much higher than that of metal/multilayer-graphene ($n > 3$) nanocomposite. (SLG: single-layer graphene; BLG: bilayer graphene; TLG: trilayer graphene.)

layers of graphene are shown in figure 3. We find that copper–graphene and nickel–graphene interfaces have similar thermal interfacial conductances. This finding is consistent with experimental results [34] that have shown that there is only a $\sim 5\%$ difference between the thermal boundary resistance between the CNT sheet and Cu, and between the CNT sheet and Ni, indicating that our results provide a reasonable qualitative model for studying the interface thermal conductance of metal–graphene nanocomposites.

Interestingly, we find that metal–single-layer graphene has excellent thermal interface conductance with a value of $\sim 500 \text{ MW m}^{-2} \text{ K}^{-1}$. The thermal interface conductance of the metal–bilayer graphene interface is about half that of the metal–single-layer-graphene interface and when the number of layers of graphene is larger than trilayer graphene, the thermal interface conductance reduces to $\sim 100 \text{ MW m}^{-2} \text{ K}^{-1}$ and there is no dependence between the number of layers of graphene and the thermal interface conductances. It is worth noting that Schmidt *et al* have shown that the metal–graphite interface has a thermal interface conductance of $40\text{--}100 \text{ MW m}^{-2} \text{ K}^{-1}$ for Au–graphite, Al–graphite and Ti–graphite interfaces at 300 K [29]. Therefore, our results indicate that the value of the thermal interface conductance for the metal–multilayer ($n > 3$) graphene interface becomes close to the experimental data of metal–graphite interfaces. An important conclusion from this finding is that nanocomposites that consist of metal and single-layer graphene should have a much higher performance than metal–multilayer graphene nanocomposites.

The thermal interface conductance is mostly influenced by the interfacial bonding as both phonon flux and the

vibrational mismatch are subject to the interfacial bond strength [32]. Hopkins *et al* have shown that the increase of the bond strength at the interface increases the graphene cross-plane velocities ($v_{c,l}$ and $v_{c,t}$) and thus increases the thermal interface conductance [32]. We attribute the higher thermal interface conductance of metal–single-layer graphene to the increase of bond strength between the metal and single-layer graphene. Note that there is only metal–carbon bonds at the metal–single-layer graphene interface, while for the case of multilayer graphene, the weak interactions between graphene sheets has a significant effect at the interface. The spring constant of the metal–carbon bond, which is computed from parameters of the LJ potential (and originally derived from quantum simulations), is about 11 times larger than the spring constant between the *c*-axis graphene sheets. Since the velocity is proportional to the square root of the spring constant, this leads to a factor of 3.32 higher for the velocity. The factor coincides with the fact that the thermal interface conductance of the metal–single-layer graphene is 3.52 times larger than that of the metal and the multilayer-graphene interface. Therefore, we propose that the metal–single-layer-graphene nanocomposite has stronger bonding strength at the metal–graphene interface, which increases the graphene cross-plane velocities and thereby leads to a higher thermal interface conductance. Note that a similar mechanism has been reported by Hopkins *et al* [32] to explain the higher thermal interface conductance resulting from chemical functionalization of graphene layers. However, we anticipate that further fundamental studies are needed to fully understand the mechanisms by which heat transfers across this interface.

4. Conclusion

We studied the thermal interfacial conductance of copper–graphene and nickel–graphene nanocomposites for different geometries, including temperature effects. The analysis with respect to the effects of the number of layers of graphene on the thermal interface conductance revealed that metal–single-layer graphene has an excellent thermal interface conductance. However, the thermal interface conductance reduces by 80% as the number of layers of graphene increases to larger than trilayer graphene. We attribute the excellent thermal interface conductance of the metal–single-layer graphene to the stronger bonding strength at the metal and single-layer-graphene interface. Our results suggest that metal–single-layer-graphene nanocomposites would be potential candidate materials for the next-generation electronic or energy devices. On the other hand, since the nickel–graphene and copper–graphene interfaces have a similar thermal interface conductance—and considering nickel has better mechanical properties and nickel–graphene has a greater cohesive energy—we anticipate that the nickel–graphene nanocomposite is a better material for electronic, structural and energy applications.

Acknowledgments

We acknowledge support from DARPA-NTI. Helpful discussions with Y Zhao and C L Chen (Teledyne Scientific) are appreciated.

References

- [1] Novoselov K S *et al* 2004 Electric field effect in atomically thin carbon films *Science* **306** 666–9
- [2] Ferrari A C *et al* 2006 Raman spectrum of graphene and graphene layers *Phys. Rev. Lett.* **97** 187401
- [3] Gupta A *et al* 2006 Raman scattering from high-frequency phonons in supported *n*-graphene layer films *Nano Lett.* **6** 2667–73
- [4] Latil S and Henrard L 2006 Charge carriers in few-layer graphene films *Phys. Rev. Lett.* **97** 036803
- [5] Aoki M and Amawashi H 2007 Dependence of band structures on stacking and field in layered graphene *Solid State Commun.* **142** 123–7
- [6] Saha S K *et al* 2008 Phonons in few-layer graphene and interplanar interaction: a first-principles study *Phys. Rev.* **78** 165421
- [7] Yan J A, Ruan W Y and Chou M Y 2008 Phonon dispersions and vibrational properties of monolayer, bilayer, and trilayer graphene: density-functional perturbation theory *Phys. Rev.* **77** 125401
- [8] Koh Y K *et al* 2010 Heat conduction across monolayer and few-layer graphenes *Nano Lett.* **10** 4363–8
- [9] Rafiee M A *et al* 2009 Buckling resistant graphene nanocomposites *Appl. Phys. Lett.* **95** 223103
- [10] Rafiee M A *et al* 2009 Enhanced mechanical properties of nanocomposites at low graphene content *ACS Nano* **3** 3884–90
- [11] Kim J *et al* 2012 Thermal and electrical conductivity of Al(OH)(3) covered graphene oxide nanosheet/epoxy composites *J. Mater. Sci.* **47** 1418–26
- [12] He F A *et al* 2011 Fabrication of hybrids based on graphene and metal nanoparticles by *in situ* and self-assembled methods *Nanoscale* **3** 1182–8
- [13] Bartolucci S F *et al* 2011 Graphene–aluminum nanocomposites *Mater. Sci. Eng. A* **528** 7933–7
- [14] Song H Y and Zha X W 2010 Mechanical properties of Ni-coated single graphene sheet and their embedded aluminum matrix composites *Commun. Theor. Phys.* **54** 143–7
- [15] Huxtable S T *et al* 2003 Interfacial heat flow in carbon nanotube suspensions *Nature Mater.* **2** 731–4
- [16] Panzer M A *et al* 2008 Thermal properties of metal-coated vertically aligned single-wall nanotube arrays *Trans. ASME, J. Heat Transfer* **130** 052401
- [17] Schmidt A J, Chen X Y and Chen G 2008 Pulse accumulation, radial heat conduction, and anisotropic thermal conductivity in pump–probe transient thermoreflectance *Rev. Sci. Instrum.* **79** 114902
- [18] Chen Z *et al* 2009 Thermal contact resistance between graphene and silicon dioxide *Appl. Phys. Lett.* **95** 161910
- [19] Daw M S and Baskes M I 1984 Embedded-atom method—derivation and application to impurities, surfaces, and other defects in metals *Phys. Rev. B* **29** 6443–53
- [20] Brenner D W *et al* 2002 A second-generation reactive empirical bond order (REBO) potential energy expression for hydrocarbons *J. Phys.: Condens. Matter* **14** 783–802
- [21] Bardotti L *et al* 1995 Experimental observation of fast diffusion of large antimony clusters on graphite surfaces *Phys. Rev. Lett.* **74** 4694–7
- [22] Guo Y F and Guo W L 2006 Structural transformation of partially confined copper nanowires inside defected carbon nanotubes *Nanotechnology* **17** 4726–30

- [23] Huang S P, Mainardi D S and Balbuena P B 2003 Structure and dynamics of graphite-supported bimetallic nanoclusters *Surf. Sci.* **545** 163–79
- [24] Plimpton S 1995 Fast parallel algorithms for short-range molecular-dynamics *J. Comput. Phys.* **117** 1–19
- [25] Müller-Plathe F 1997 A simple nonequilibrium molecular dynamics method for calculating the thermal conductivity *J. Chem. Phys.* **106** 6082–5
- [26] Gao F, Qu J M and Yao M 2011 Interfacial thermal resistance between metallic carbon nanotube and Cu substrate *J. Appl. Phys.* **110** 124314
- [27] Duda J C *et al* 2009 Extension of the diffuse mismatch model for thermal boundary conductance between isotropic and anisotropic materials *Appl. Phys. Lett.* **95** 031912
- [28] Hirotani J *et al* 2011 Thermal boundary resistance between the end of an individual carbon nanotube and a Au surface *Nanotechnology* **22** 315702
- [29] Schmidt A J *et al* 2010 Thermal conductance and phonon transmissivity of metal–graphite interfaces *J. Appl. Phys.* **107** 104907
- [30] Duda J C *et al* 2010 Inelastic phonon interactions at solid-graphite interfaces *Superlattices Microstruct.* **47** 550–5
- [31] Swartz E T and Pohl R O 1989 Thermal-boundary resistance *Rev. Mod. Phys.* **61** 605–68
- [32] Hopkins P E *et al* 2012 Manipulating thermal conductance at metal–graphene contacts via chemical functionalization *Nano Lett.* **12** 590–5
- [33] Giannozzi P *et al* 2009 QUANTUM ESPRESSO: a modular and open-source software project for quantum simulations of materials *J. Phys.: Condens. Matter* **21** 395502
- [34] Li Q W, Liu C H and Fan S S 2009 Thermal boundary resistances of carbon nanotubes in contact with metals and polymers *Nano Lett.* **9** 3805–9
- [35] www.quantum-espresso.org